

Low Probability of Intercept Antenna Array Beamforming

Daniel E. Lawrence, *Member, IEEE*

Abstract—A novel transmit array beamforming approach is introduced that offers low probability of intercept (LPI) for surveillance radar systems employing phased array antennas. Radar systems are often highly visible to intercept receivers due to the inherent two-way versus one-way propagation loss. In this paper, the traditional high-gain antenna beam scanned across a search region is replaced with a series of low-gain, spoiled beams. Keeping the transmit antenna gain low reduces the radar visibility, but the radar's antenna performance remains unchanged as the original high-gain beam can be formed by processing the set of spoiled beams. Large transient power density radiated in a traditional scan is replaced with low power density persistently radiated at the target throughout the scan time. The detection performance of the radar is not affected since the total energy on the target is the same. Derivation of the complex weights to synthesize the high-gain patterns from the low-gain basis patterns is presented for both one-way and two-way beam patterns.

Index Terms—Antenna arrays, beamforming, low-probability of intercept, radar.

I. INTRODUCTION

ON the modern battlefield, active surveillance radars are highly vulnerable to detection and exploitation by opposing forces. The ongoing battle between radar systems and the electronic devices used to exploit, degrade, or prevent radar operation has been termed electronic warfare (EW) and is divided into two broad categories: 1) Electronic support measures (ESM) and 2) electronic counter-measures (ECM). The distinction between the two is simply that ESM is typically used to search, identify, record, and analyze radiated radar signals for potential exploitation during military operations, while ECM involves the active approaches taken to degrade radar's effectiveness [1], [2]. An ESM device could be realized as a basic radar warning receiver (RWR), but ESM is often cast in terms of the broader category of electronic intelligence (ELINT) encompassing both tactical and strategic information gathering [3], [4]. In this paper, the term ESM is used to denote any EW device used to intercept the radar transmission and potentially enable harmful ECM techniques.

In light of the significant threat presented by ESM receivers, there has been a growing trend towards the development of

low probability of intercept (LPI) radar systems. The underlying weakness of any monostatic radar system, whose theoretical performance is dictated by the radar range equation, is the classic two-way ($1/R^4$) versus one-way ($1/R^2$) propagation loss experienced by the radar and intercept receiver, respectively. The ESM receiver always has the upper hand when it comes to received power, and in most cases will be able to intercept the radar transmission well beyond the radar's detection range. To overcome the inherent disadvantage of the radar, a number of techniques have been developed to reduce the radar visibility and enhance LPI performance. Many of these techniques are well documented in the open literature [5]–[15]. In general, the capacity to reduce radar visibility relies on three key areas: 1) spreading the energy in time with high duty cycle waveforms; 2) spreading the energy in frequency with wide bandwidth waveforms; and 3) spreading the energy in space through broad transmitter antenna beams. Often combinations of these techniques are used together to improve performance.

Perhaps the most common LPI technique employs the use of high duty cycle, wideband waveforms. Phase modulated CW, FMCW, frequency hopping, and random waveforms have all been reported in terms of their LPI qualities [16]–[23]. There is an upper limit, however, on the bandwidth extent that is feasible to spread the transmitted waveform. If the bandwidth of the radar waveform is increased such that individual scatterers on the target are resolved in range, then the detection performance of the radar becomes compromised offsetting the benefits of LPI [24]. In conjunction with waveform design, transmit antenna modifications can also improve LPI performance. A novel switched antenna approach, called antenna hopping, has been proposed [25]. Fielded radar systems often use irregular scan patterns to reduce susceptibility to receivers that use scan rate information for detection. Additionally, suppressing antenna sidelobe levels reduces the probability of being detected in a sidelobe region. Even with suppressed sidelobes, however, a high gain scanning main beam is still likely to be detected. Thus, it is desirable to keep the transmit gain low to reduce the peak power available to an ESM receiver. To accomplish this, a corresponding increase in integration time is needed to compensate for the lost gain. In [26] a technique is introduced that applies a broad beam transmit antenna to reduce the peak radiated power and is referred to as the omnidirectional LPI (OLPI) radar. Specifically, an omnidirectional transmit antenna is used in conjunction with multiple, narrow beam receive antenna channels to cover the desired surveillance field of view. To make up for the lost transmit gain, the integration time is increased to be the same as what the scan time would have been for a traditionally scanned, high-gain transmit antenna

Manuscript received October 06, 2009; revised February 12, 2010; accepted March 20, 2010. Date of publication June 14, 2010; date of current version September 03, 2010.

The author is with the Phase IV Systems Operation of Technology Service Corporation, Huntsville, AL 35802 USA (e-mail: dlawrence@phaseiv.com).

Color versions of one or more of the figures in this paper are available online at <http://ieeexplore.ieee.org>.

Digital Object Identifier 10.1109/TAP.2010.2052573

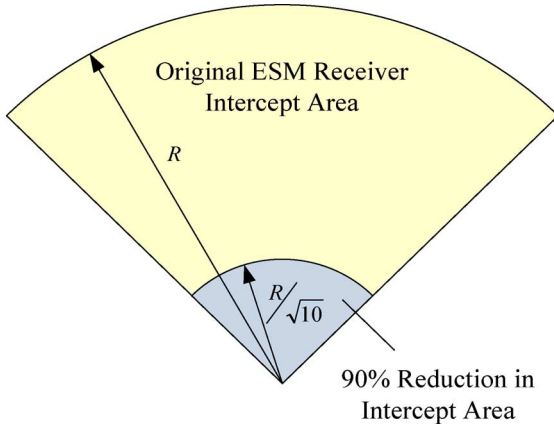


Fig. 1. Reduction of ESM receiver intercept area when the peak radar transmit antenna gain is reduced by 10 dB.

beam [27]–[29]. The main drawback of this approach is the need for simultaneous receive beams which, for large arrays, significantly increases hardware complexity.

In this paper, a beam-spoiling technique is introduced to provide good LPI performance that can be implemented with only a single receive antenna channel without sacrificing antenna gain. Rather than scanning a high-gain transmit beam, a series of low-gain spoiled beams covering the desired surveillance region are formed sequentially. The sequence of low-gain beams comprise a set of basis patterns that can then be weighted and coherently combined to form an ensemble of high-gain beams scanned across the prescribed field of view. In this way, the peak power radiated in any direction is significantly reduced while maintaining the same antenna performance as a traditional surveillance radar with scanned high-gain antenna. In essence, low power persistently radiated over the surveillance area has replaced the transient high power sweep. To the author's knowledge, the LPI beamformer technique presented here is novel and offers the potential to significantly reduce the visibility of modern surveillance radar systems.

It should be noted that a radar system enhanced by the LPI technique described here still might not be able to detect a target before being detected itself. Rather, the term LPI is used to denote that the intercept range of an ESM receiver has been greatly reduced or, equivalently, that the probability of intercept has been reduced at a particular standoff range. The potential impact of an LPI beamformer is illustrated in Fig. 1. It is shown that a reduction of 10 dB in the radar's transmit antenna gain brings in the maximum intercept range of the ESM receiver by a factor of $1/\sqrt{10}$, equating to a factor of 10 reduction in the intercept area. Using the methodology presented in this paper, however, the radar detection range remains unchanged while limiting the intercept area of the ESM receiver.

In what follows, a novel technique for spoiling the radar antenna pattern through judicious choice of phase shifter settings is described with the goal of enhancing LPI performance. The principle is initially applied in Section II to a one-way pattern in order to derive the fundamental beam spreading and recombination equations. It is demonstrated that complex weights can be applied to the set of spread patterns to synthesize any of

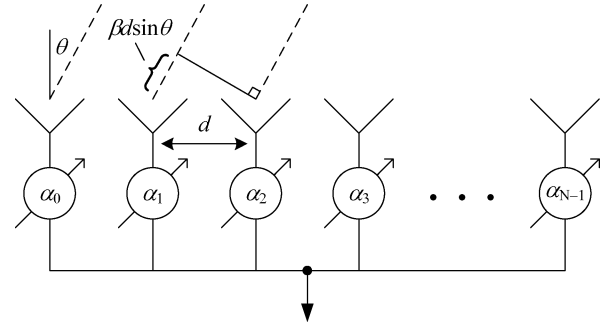


Fig. 2. N -element linear phased array antenna. α_n denotes the phase shifter setting for the n th element.

the desired high-gain, scanned patterns. Many radar applications use the same antenna for transmit and receive and, thus, the equations are extended in Section III for the two-way antenna pattern. Finally, an implementation discussion is provided in Section IV followed by a summary of the work in Section V.

II. ONE-WAY PATTERN SYNTHESIS

In this section, the high-gain pattern synthesis approach is presented for a set of low-gain transmit beams. When the pattern is only affected on transmit, it is referred to as a one-way synthesis. An example application of the one-way synthesis would be a spoiled-beam transmit array combined with multiple simultaneous receive beams. Consider the linear antenna array shown in Fig. 2. For a linear array of N elements with uniform excitation, the far-field radiation pattern is expressed

$$f_0(\theta) = 1 + e^{j\beta d \sin \theta} + e^{j2\beta d \sin \theta} + \dots + e^{j(N-1)\beta d \sin \theta} \quad (1)$$

where $\beta = 2\pi/\lambda$ is the free-space propagation constant, d is the array element spacing, and θ is the spatial angle measured from the array broadside. It is convenient for the following development to make a substitution for the relative phase between elements

$$\psi = \beta d \sin \theta. \quad (2)$$

The fundamental array pattern is now written

$$f_0(\psi) = 1 + e^{j\psi} + e^{j2\psi} + \dots + e^{j(N-1)\psi}. \quad (3)$$

The pattern in (3) is characterized by a dominant mainlobe with high gain directed broadside to the array. The high-gain pattern can be scanned by applying a linear phase progression across the array. The set of scanned patterns, with the fundamental phase scan $\gamma = 2\pi/N$ is written

$$\begin{aligned} f_1(\psi) &= 1 + e^{j\gamma} e^{j\psi} + e^{j2\gamma} e^{j2\psi} + \dots + e^{j(N-1)\gamma} e^{j(N-1)\psi} \\ f_2(\psi) &= 1 + e^{j2\gamma} e^{j\psi} + e^{j4\gamma} e^{j2\psi} + \dots + e^{j2(N-1)\gamma} e^{j(N-1)\psi} \\ f_3(\psi) &= 1 + e^{j3\gamma} e^{j\psi} + e^{j6\gamma} e^{j2\psi} + \dots + e^{j3(N-1)\gamma} e^{j(N-1)\psi} \\ &\vdots \\ f_{N-1}(\psi) &= 1 + e^{j(N-1)\gamma} e^{j\psi} + \dots + e^{j(N-1)(N-1)\gamma} e^{j(N-1)\psi}. \end{aligned} \quad (4)$$

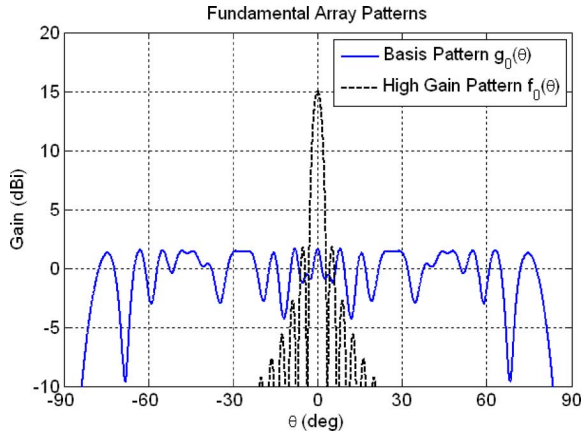


Fig. 3. Fundamental basis pattern and broadside high-gain pattern comparison for a 32 element linear phased array.

For LPI applications, it is desirable to form high-gain patterns by a linear combination of low-gain basis patterns. A fundamental basis pattern can be formed by applying a select phase shift to each array element. The set of phase shift values is chosen to create a low gain, “spoiled” beam pattern. The fundamental basis pattern is written

$$g_0(\psi) = 1 + e^{j\alpha_1} e^{j\psi} + e^{j\alpha_2} e^{j2\psi} + \dots + e^{j\alpha_{N-1}} e^{j(N-1)\psi}. \quad (5)$$

An example low-gain basis pattern for a 32 element array is shown in Fig. 3. This pattern is formed by computer optimization of a quadratic phase shift variation across the elements where the goal is to minimize the gain. Details of the phase shifter settings used for this paper are provided in the Appendix. Other techniques to form broad beam patterns are given in [30]–[33]. The peak gain is only 1.7 dB compared to 15 dB for the fundamental high-gain pattern. Additional patterns are formed by applying a linear phase progression to the fundamental basis pattern. The phase progression is in increments of γ for the 1st pattern, 2γ for the 2nd pattern and so on. This results in $N - 1$ steered versions of the fundamental pattern. There are other possibilities for choosing the remaining basis patterns, but steered versions of the fundamental ensure linear independence. The set of basis patterns derived from the fundamental are expressed

$$\begin{aligned} g_1(\psi) &= 1 + e^{j\alpha_1} e^{j\gamma} e^{j\psi} + \dots + e^{j\alpha_{N-1}} e^{j(N-1)\gamma} e^{j(N-1)\psi} \\ g_2(\psi) &= 1 + e^{j\alpha_1} e^{j2\gamma} e^{j\psi} + \dots + e^{j\alpha_{N-1}} e^{j2(N-1)\gamma} e^{j2(N-1)\psi} \end{aligned}$$

$$\begin{aligned} &\dots + e^{j\alpha_{N-1}} e^{j2(N-1)\gamma} e^{j(N-1)\psi} \\ g_3(\psi) &= 1 + e^{j\alpha_1} e^{j3\gamma} e^{j\psi} + \dots + e^{j\alpha_{N-1}} e^{j3(N-1)\gamma} e^{j(N-1)\psi} \\ &\vdots \\ g_{N-1}(\psi) &= 1 + e^{j\alpha_1} e^{j(N-1)\gamma} e^{j\psi} + \dots + e^{j\alpha_{N-1}} e^{j(N-1)(N-1)\gamma} e^{j(N-1)\psi}. \quad (6) \end{aligned}$$

Since the basis patterns are steered versions of the fundamental, they all exhibit low gain and broad beamwidth. The ultimate goal of this development is to write the set of high-gain, scanned patterns as a linear combination of the low-gain basis patterns, $g_n(\psi)$. Suppose the original broadside pattern in (3) can be written as a summation of all N basis patterns where the n th basis pattern is weighted by the complex coefficient $w_{0,n}$

$$f_0(\psi) = w_{0,0}g_0(\psi) + w_{0,1}g_1(\psi) + w_{0,2}g_2(\psi) + \dots + w_{0,N-1}g_{N-1}(\psi). \quad (7)$$

Furthermore, suppose the remaining scanned high-gain patterns can also be formed by linear combinations of the basis patterns with the appropriate complex coefficients, $w_{m,n}$

$$\begin{aligned} f_1(\psi) &= w_{1,0}g_0(\psi) + w_{1,1}g_1(\psi) + \dots + w_{1,N-1}g_{N-1}(\psi) \\ f_2(\psi) &= w_{2,0}g_0(\psi) + w_{2,1}g_1(\psi) + \dots + w_{2,N-1}g_{N-1}(\psi) \\ &\vdots \\ f_{N-1}(\psi) &= w_{N-1,0}g_0(\psi) + w_{N-1,1}g_1(\psi) + \dots + w_{N-1,N-1}g_{N-1}(\psi). \quad (8) \end{aligned}$$

By expanding the high-gain pattern and basis patterns in (7) and equating equal powers of $e^{j\psi}$, a matrix equation can be set up for the coefficients $w_{0,n}$

$$A \cdot \begin{bmatrix} w_{0,0} \\ w_{0,1} \\ w_{0,2} \\ \vdots \\ w_{0,N-1} \end{bmatrix} = \begin{bmatrix} 1 \\ 1 \\ 1 \\ \vdots \\ 1 \end{bmatrix} \quad (9)$$

where the matrix A is defined in (10), shown at the bottom of the page. Using (8), the remaining set of $N - 1$ matrix equations can be written for the complex coefficients to form each of the remaining $N - 1$ scanned beams

$$A = \begin{bmatrix} 1 & 1 & 1 & \dots & 1 \\ e^{j\alpha_1} & e^{j(\alpha_1+\gamma)} & e^{j(\alpha_1+2\gamma)} & \dots & e^{j[\alpha_1+(N-1)\gamma]} \\ e^{j\alpha_2} & e^{j(\alpha_2+2\gamma)} & e^{j(\alpha_2+4\gamma)} & \dots & e^{j[\alpha_2+2(N-1)\gamma]} \\ & \vdots & & \ddots & \vdots \\ e^{j\alpha_{N-1}} & e^{j[\alpha_{N-1}+(N-1)\gamma]} & e^{j[\alpha_{N-1}+2(N-1)\gamma]} & \dots & e^{j[\alpha_{N-1}+(N-1)(N-1)\gamma]} \end{bmatrix}. \quad (10)$$

$$\begin{aligned}
 A \cdot \begin{bmatrix} w_{1,0} \\ w_{1,1} \\ w_{1,2} \\ \vdots \\ w_{1,N-1} \end{bmatrix} &= \begin{bmatrix} 1 \\ e^{j\gamma} \\ e^{j2\gamma} \\ \vdots \\ e^{j(N-1)\gamma} \end{bmatrix} \\
 A \cdot \begin{bmatrix} w_{2,0} \\ w_{2,1} \\ w_{2,2} \\ \vdots \\ w_{2,N-1} \end{bmatrix} &= \begin{bmatrix} 1 \\ e^{j2\gamma} \\ e^{j4\gamma} \\ \vdots \\ e^{j2(N-1)\gamma} \end{bmatrix} \\
 &\vdots \\
 A \cdot \begin{bmatrix} w_{N-1,0} \\ w_{N-1,1} \\ w_{N-1,2} \\ \vdots \\ w_{N-1,N-1} \end{bmatrix} &= \begin{bmatrix} 1 \\ e^{j(N-1)\gamma} \\ e^{j2(N-1)\gamma} \\ \vdots \\ e^{j(N-1)(N-1)\gamma} \end{bmatrix}. \quad (11)
 \end{aligned}$$

The equation set (9) and (11) can be combined into a single $N \times N$ matrix equation to solve for all coefficients simultaneously

$$\begin{aligned}
 &\begin{bmatrix} w_{0,0} & w_{1,0} & w_{2,0} & \cdots & w_{N-1,0} \\ w_{0,1} & w_{1,1} & w_{2,1} & \cdots & w_{N-1,1} \\ w_{0,2} & w_{1,2} & w_{2,2} & \cdots & w_{N-1,2} \\ \vdots & \vdots & \vdots & \ddots & \vdots \\ w_{0,N-1} & w_{1,N-1} & w_{2,N-1} & \cdots & w_{N-1,N-1} \end{bmatrix} \\
 &= A^{-1} \cdot \begin{bmatrix} 1 & 1 & 1 & \cdots & 1 \\ 1 & e^{j\gamma} & e^{j2\gamma} & \cdots & e^{j(N-1)\gamma} \\ 1 & e^{j2\gamma} & e^{j4\gamma} & \cdots & e^{j2(N-1)\gamma} \\ \vdots & \vdots & \vdots & \ddots & \vdots \\ 1 & e^{j(N-1)\gamma} & e^{j2(N-1)\gamma} & \cdots & e^{j(N-1)(N-1)\gamma} \end{bmatrix}. \quad (12)
 \end{aligned}$$

Using the coefficients calculated in (12) in the synthesis (7) and (8) allows high-gain patterns to be formed by linear combinations of the N basis patterns. It should be noted that once the set of basis patterns have been formed, all N steered high-gain patterns can be synthesized at once. Fig. 4 demonstrates the high-gain patterns of a 32 element array steered to 0 deg, +30 deg, and -30 deg. The patterns are formed by linear combination of the 32 basis patterns. Again, any of the 32 high-gain patterns can be formed once the basis patterns are available.

III. TWO-WAY PATTERN SYNTHESIS

When the same antenna array is used for both transmit and receive, the one-way pattern formation is not sufficient since the target return is scaled by the square of the pattern. The synthesis of the two-way pattern is slightly more complex and is achieved by a linear combination of two-way basis patterns. In order to represent the two-way pattern as a summation of powers of $e^{j\psi}$, the squared version of the broadside high-gain pattern of (3) is written

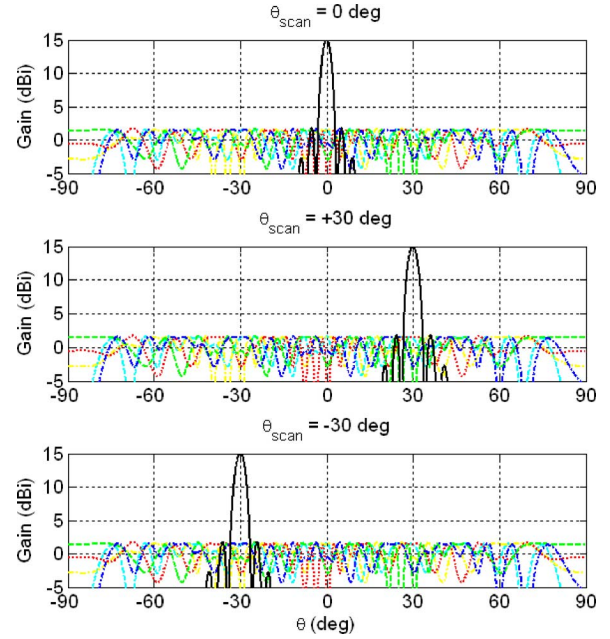


Fig. 4. Illustration of scanned high-gain patterns (solid line) formed by linear combinations of 32 low-gain basis patterns (dashed lines) for a 32 element linear array.

$$\begin{aligned}
 f_0^2(\psi) &= \left[\sum_{n=0}^{N-1} e^{jn\psi} \right]^2 = \sum_{n=0}^{N-1} e^{jn\psi} \cdot \sum_{m=0}^{N-1} e^{jm\psi} \\
 &= \sum_{n=0}^{N-1} \sum_{m=0}^{N-1} e^{j(n+m)\psi}. \quad (13)
 \end{aligned}$$

If we let $k = m + n$, it is straightforward to show that (13) can be expressed

$$\begin{aligned}
 f_0^2(\psi) &= \sum_{k=0}^{N-1} e^{jk\psi} \cdot (k+1) + \sum_{k=N}^{2N-2} e^{jk\psi} \cdot (2N-1-k) \\
 &= \sum_{k=0}^{2N-2} e^{jk\psi} \cdot T_k \quad (14)
 \end{aligned}$$

where

$$T_k = \begin{cases} k+1, & \text{for } k < N \\ 2N-1-k, & \text{for } k \geq N \end{cases}. \quad (15)$$

Scanned versions of the squared high-gain pattern, having a fundamental phase scan $\gamma = 2\pi/(N-1/2)$, can be written

$$\begin{aligned}
 f_1^2(\psi) &= \left[\sum_{n=0}^{N-1} e^{jn\gamma} e^{jn\psi} \right]^2 = \sum_{k=0}^{2N-2} e^{jk\psi} \cdot e^{jk\gamma} T_k \\
 f_2^2(\psi) &= \left[\sum_{n=0}^{N-1} e^{jn2\gamma} e^{jn\psi} \right]^2 = \sum_{k=0}^{2N-2} e^{jk\psi} \cdot e^{jk2\gamma} T_k \\
 &\vdots \\
 f_{2N-2}^2(\psi) &= \left[\sum_{n=0}^{N-1} e^{jn(2N-2)\gamma} e^{jn\psi} \right]^2 \\
 &= \sum_{k=0}^{2N-2} e^{jk\psi} \cdot e^{jk(2N-2)\gamma} T_k. \quad (16)
 \end{aligned}$$

Note that there are $2N - 1$ scanned patterns corresponding to the number of $e^{jk\psi}$ terms in the squared pattern expansion. Fig. 5 shows several scanned high-gain patterns for a 32 element linear array. The fundamental two-way pattern can be synthesized by a weighted summation of two-way basis patterns

$$f_0^2(\psi) = w_{0,0}g_0^2(\psi) + w_{0,1}g_1^2(\psi) + \dots + w_{0,2N-2}g_{2N-2}^2(\psi). \quad (17)$$

Similarly, scanned versions of the high-gain pattern can also be synthesized

$$\begin{aligned} f_1^2(\psi) &= w_{1,0}g_0^2(\psi) + w_{1,1}g_1^2(\psi) + \dots + w_{1,2N-2}g_{2N-2}^2(\psi) \\ f_2^2(\psi) &= w_{2,0}g_0^2(\psi) + w_{2,1}g_1^2(\psi) + \dots + w_{2,2N-2}g_{2N-2}^2(\psi) \\ &\vdots \\ f_{2N-2}^2(\psi) &= w_{2N-2,0}g_0^2(\psi) + w_{2N-2,1}g_1^2(\psi) + \dots + w_{2N-2,2N-2}g_{2N-2}^2(\psi). \end{aligned} \quad (18)$$

Since the squared basis patterns are used to form the squared high-gain pattern, it is necessary to represent the squared basis patterns in a summation of $e^{jk\psi}$ terms. The squared fundamental basis pattern can be written

$$\begin{aligned} g_0^2(\psi) &= \left[\sum_{n=0}^{N-1} e^{j\alpha_n} e^{jn\psi} \right]^2 = \sum_{n=0}^{N-1} e^{j\alpha_n} e^{jn\psi} \cdot \sum_{m=0}^{N-1} e^{j\alpha_m} e^{jm\psi} \\ &= \sum_{n=0}^{N-1} \sum_{m=0}^{N-1} e^{j(n+m)\psi} \cdot e^{j(\alpha_n + \alpha_m)}. \end{aligned} \quad (19)$$

By letting $k = m + n$, (19) can be rewritten as a summation of weighted powers of $e^{j\psi}$

$$\begin{aligned} g_0^2(\psi) &= \sum_{k=0}^{N-1} e^{jk\psi} \sum_{n=0}^k e^{j(\alpha_n + \alpha_{k-n})} \\ &\quad + \sum_{k=N}^{2N-2} e^{jk\psi} \sum_{n=k-(N-1)}^{N-1} e^{j(\alpha_n + \alpha_{k-n})} \\ &= \sum_{k=0}^{2N-2} e^{jk\psi} X_k \end{aligned} \quad (20)$$

where

$$X_k = \begin{cases} \sum_{n=0}^k e^{j(\alpha_n + \alpha_{k-n})}, & \text{for } k < N \\ \sum_{n=k-(N-1)}^{N-1} e^{j(\alpha_n + \alpha_{k-n})}, & \text{for } k \geq N \end{cases}. \quad (21)$$

The fundamental two-way basis pattern together with the broadside high-gain pattern are shown in Fig. 6 for a 32 element array. Although the two-way basis patterns are shown here, keep in

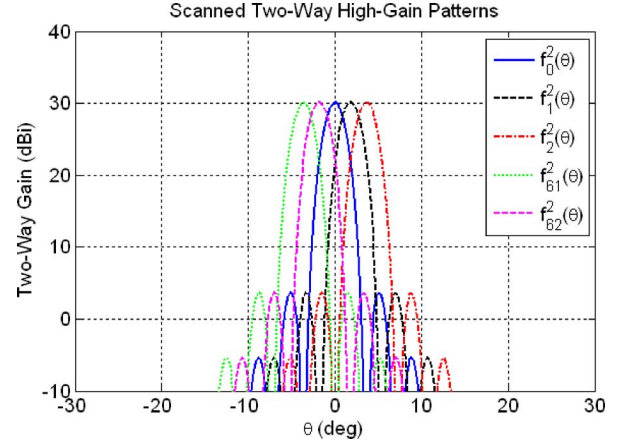


Fig. 5. Selected scanned two-way, high-gain patterns for a 32 element linear array. The fundamental scan angle is $\theta_s = 3.6$ deg. The entire constellation of 63 scanned patterns would fill the entire angular region from $+90$ deg to $+90$ deg.

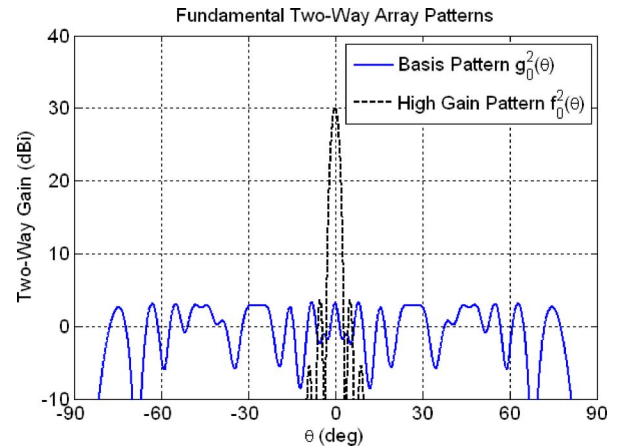


Fig. 6. Fundamental two-way basis pattern and broadside high-gain pattern comparison for a 32 element linear phased array.

mind that for LPI performance assessment we should only consider the transmit pattern which remains a one-way pattern.

Similarly, the remaining squared basis patterns can be written

$$\begin{aligned} g_1^2(\psi) &= \left[\sum_{n=0}^{N-1} e^{j\alpha_n} e^{jn\gamma} e^{jn\psi} \right]^2 = \sum_{k=0}^{2N-2} e^{jk\psi} \cdot e^{jk\gamma} X_k \\ g_2^2(\psi) &= \left[\sum_{n=0}^{N-1} e^{j\alpha_n} e^{jn2\gamma} e^{jn\psi} \right]^2 = \sum_{k=0}^{2N-2} e^{jk\psi} \cdot e^{jk2\gamma} X_k \\ &\vdots \\ g_{2N-2}^2(\psi) &= \left[\sum_{n=0}^{N-1} e^{j\alpha_n} e^{jn(2N-2)\gamma} e^{jn\psi} \right]^2 \\ &= \sum_{k=0}^{2N-2} e^{jk\psi} \cdot e^{jk(2N-2)\gamma} X_k \end{aligned} \quad (22)$$

where X_k is defined in (21). Substituting (14), (20), and (22) into the pattern synthesis equation of (17) and equating equal powers of $e^{j\psi}$ results in $2N - 1$ equations for the complex basis coefficients, $w_{0,n}$

$$\frac{T_k}{X_k} = w_{0,0} + w_{0,1}e^{jk\gamma} + w_{0,2}e^{jk2\gamma} + \dots + w_{0,2N-2}e^{jk(2N-2)\gamma} \quad \text{for } k = 0, 1, \dots, 2N - 2. \quad (23)$$

In matrix form, the set of equations in (23) can be written

$$B \cdot \begin{bmatrix} w_{0,0} \\ w_{0,1} \\ w_{0,2} \\ \vdots \\ w_{0,2N-2} \end{bmatrix} = \begin{bmatrix} \frac{T_0}{X_0} \\ \frac{T_1}{X_1} \\ \frac{T_2}{X_2} \\ \vdots \\ \frac{T_{2N-2}}{X_{2N-2}} \end{bmatrix} \quad (24)$$

where the matrix B is defined to be

$$B = \begin{bmatrix} 1 & 1 & 1 & \dots & 1 \\ 1 & e^{j\gamma} & e^{j2\gamma} & \dots & e^{j(2N-2)\gamma} \\ 1 & e^{j2\gamma} & e^{j4\gamma} & \dots & e^{j2(2N-2)\gamma} \\ \vdots & \vdots & \vdots & \ddots & \vdots \\ 1 & e^{j(2N-2)\gamma} & e^{j(2N-2)2\gamma} & \dots & e^{j(2N-2)^2\gamma} \end{bmatrix}. \quad (25)$$

Solving for the coefficients to form the remaining set of scanned patterns in (18) is accomplished through a combined matrix equation which allows simultaneous solution for the pattern weights, see (26) at the bottom of the page. Using the weights calculated in (26) and the synthesis equations of (17) and (18), any of the high-gain patterns can be synthesized by linear combinations of the basis patterns. Fig. 7 demonstrates the high-gain patterns of a 32 element array steered to 0 deg, +30 deg, and -30 deg where the patterns are formed by linear combination of the 63 basis patterns.

IV. IMPLEMENTATION

Some discussion is in order on the practical implementation of the LPI beamforming approach described in this paper. The theoretical antenna performance that can be achieved after generating the set of high-gain beams from the low-gain basis patterns is the same as an un-spoiled, high-gain beam scanned over the same coverage area. Transient peak power is traded for sustained low power on the target over the search region, resulting in equivalent total energy on the target. Since the phase relation-

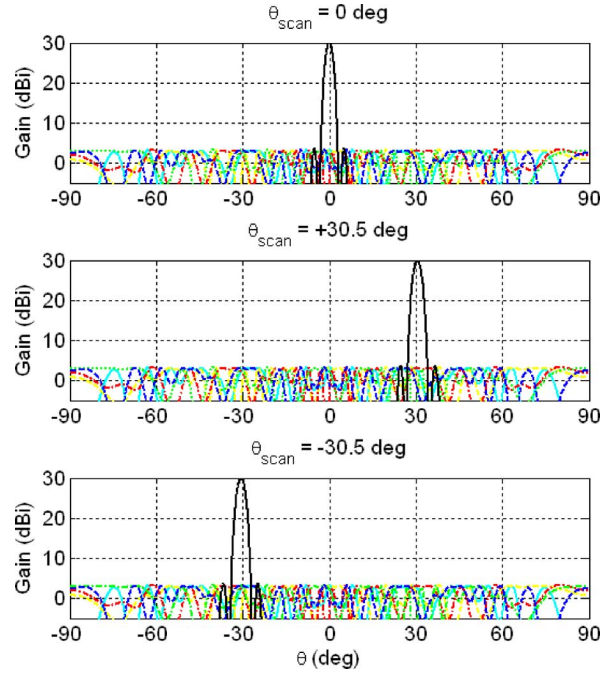


Fig. 7. Illustration of scanned two-way, high-gain patterns (solid line) formed by linear combinations of 32 low-gain basis patterns (dashed lines) for a 32 element linear array.

ship between basis patterns is important, the target must remain coherent over the scan time of the radar. For long scan times, this may require motion compensation for the target dynamics. The coherency requirement is the same as that required by traditional Doppler processing over the same scan time interval. Also, if the radar system is limited by receiver thermal noise, rather than ground clutter for example, the two-way beam pattern formulation may not have sufficient integration time to overcome the two-way gain loss. The pattern performance remains the same, but the resulting signal-to-noise will be lower than if a one-way pattern formulation combined with a multi-channel receiver having high gain were used on receive.

In order to fully utilize the LPI beamforming approach in a particular radar system, the beam switching methodology must first be integrated with the radar waveform. A vast number of waveforms exist for many different radar performance objectives, and it is beyond the scope of this paper to address them all. Instead, an implementation using a standard pulsed waveform is suggested. Specifically, consider a waveform consisting

$$\begin{bmatrix} w_{0,0} & w_{1,0} & w_{2,0} & \dots & w_{2N-2,0} \\ w_{0,1} & w_{1,1} & w_{2,1} & \dots & w_{2N-2,1} \\ w_{0,2} & w_{1,2} & w_{2,2} & \dots & w_{2N-2,2} \\ \vdots & \vdots & \vdots & \ddots & \vdots \\ w_{0,2N-2} & w_{1,2N-2} & w_{2,2N-2} & \dots & w_{2N-2,2N-2} \end{bmatrix} = B^{-1} \cdot \begin{bmatrix} \frac{T_0}{X_0} & \frac{T_0}{X_0} & \frac{T_0}{X_0} & \dots & \frac{T_0}{X_0} \\ \frac{T_1}{X_1} & \frac{T_1 e^{j\gamma}}{X_1} & \frac{T_1 e^{j2\gamma}}{X_1} & \dots & \frac{T_1 e^{j(2N-2)\gamma}}{X_1} \\ \frac{T_2}{X_2} & \frac{T_2 e^{j2\gamma}}{X_2} & \frac{T_2 e^{j4\gamma}}{X_2} & \dots & \frac{T_2 e^{j2(2N-2)\gamma}}{X_2} \\ \vdots & \vdots & \vdots & \ddots & \vdots \\ \frac{T_{2N-2}}{X_{2N-2}} & \frac{T_{2N-2} e^{j(2N-2)\gamma}}{X_{2N-2}} & \frac{T_{2N-2} e^{j(2N-2)2\gamma}}{X_{2N-2}} & \dots & \frac{T_{2N-2} e^{j(2N-2)^2\gamma}}{X_{2N-2}} \end{bmatrix}. \quad (26)$$

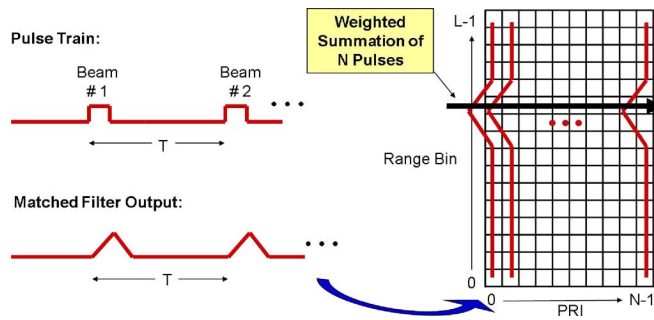


Fig. 8. Illustration of processing architecture to implement beamforming approach. Complex weights are applied to the matched filter output before summing across multiple PRIs.

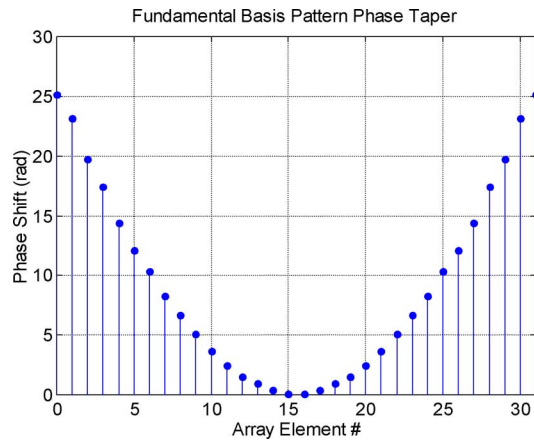


Fig. 9. Phase taper for the fundamental low-gain basis pattern. Note that the phase shift values are in radians and have not been wrapped.

of N consecutive pulses separated by the pulse repetition interval (PRI). A notional block diagram of a digital processing architecture for this waveform is shown in Fig. 8. Here each pulse is transmitted and received using phase-shifter settings for a particular low-gain basis pattern: beam #1 for pulse #1, beam #2 for pulse #2, and so on. Each pulse is processed through a matched filter and then fills a corner-turn memory where the rows represent different range samples and the columns of the corner-turn are used to store sequential PRI data. The complex weights calculated in (12) or (26) are applied across PRI samples and summed. For a particular set of weights, the weighted summation forms the equivalent range return of a single high-gain beam. Note that once the data is collected, N separate returns can be formed simultaneously by applying weights from each column of (12) or (26). There is no extra scan time required when compared to the traditional method of using N separate high-gain beams that scan across the same region. Other LPI beamforming implementations are possible and could potentially be integrated with waveforms also designed for LPI performance. This represents a promising area of future work.

V. CONCLUSION

In this paper, a novel transmit beamforming approach is presented that provides an LPI alternative to a traditional scanned high-gain antenna beam. Both one-way and two-way high-gain patterns can be synthesized by weighted combination

of spoiled, low-gain basis patterns. The obvious advantage of the technique presented here is the significant reduction in ESM intercept range that accompanies the reduction in peak transmit gain. Although peak gain is reduced, the target detection performance of the LPI beamforming approach can be made identical to that of a traditional high-gain beam since the total energy on the target is the same. The advantages of using LPI beamforming come at the cost of increased memory and processing requirements as well as restrictions on the target dynamics since the target must remain coherent over the entire scan time. Overall, the technique offers a promising tool that can possibly be combined with other LPI waveform techniques to reduce radar susceptibility and visibility in the ongoing LPI battle.

APPENDIX

A low-gain basis pattern can be implemented by selecting phase shifter values that provide a broad, spoiled beam. A uniform or linear phase variation across the array results in a high-gain beam steered in angle proportional to the slope of the phase variation. Alternatively, by introducing a quadratic phase variation, the beam becomes de-focused and the gain of the array is reduced. In this paper, the phase shifter values are selected by randomly choosing a quadratic phase slope across the array. Then, using the randomly selected quadratic phase as a starting value, a multi-dimensional gradient search routine is used to minimize the gain of the array. Minimizing the gain ensures that a broad beam is achieved. The specific phase shifter settings used for the fundamental basis pattern described in this paper are given by

$$\begin{aligned} & \{\alpha_0, \alpha_1, \dots, \alpha_{15}\} \\ & = \{25.1327, 23.1712, 19.7224, 17.4168, 14.3737, 12.0629 \\ & \quad 10.3295, 8.3138, 6.6861, 5.0579, 3.6830, 2.4497 \\ & \quad 1.5341, 0.9522, 0.4120, 0.0997\}. \end{aligned}$$

These phase values are in radians. The values α_{16} through α_{31} are the same as above but in reverse order. This gives a symmetric array excitation. A plot of the phase shifter values is shown in Fig. 9 illustrating the quadratic nature of the phase. Another viable option is to randomly select the array phase shifter settings and then minimize the gain using a multi-dimensional gradient search.

REFERENCES

- [1] D. C. Schlehler, *Introduction to Electronic Warfare*. Boston, MA: Artech House, 1986.
- [2] M. Skolnik, *Radar Handbook*, 2nd ed. New York: McGraw-Hill, 1990.
- [3] J. Tsui, *Microwave Receivers With Electronic Warfare Applications*. New York: Wiley, 1986.
- [4] R. G. Wiley, *Electronic Intelligence: The Interception of Radar Signals*. Norwood, MA: Artech House, 1985.
- [5] A. G. Stove, A. L. Hume, and C. J. Baker, "Low probability of intercept radar strategies," *IEEE Proceedings-Radar Sonar and Navigation*, vol. 151, no. 5, pp. 249–260, Oct. 2004.
- [6] G. Schrick and R. Wiley, "Interception of LPI radar signals," in *Proc. IEEE Int. Radar Conf.*, 1990, pp. 108–111.
- [7] G. T. O'Reilly, T. C. Pierce, and R. R. McElroy, "Track-while-scan quiet radar," in *Proc. 15th Annu. Electronics and Aerospace Systems Conf.*, Washington, DC, Sep. 20–22, 1982, pp. 369–374.

- [8] A. G. Stove, "Radar and ESM: The current state of the LPI battle," presented at the 1st EMRS DTC Technical Conf., Edinburgh, 2004.
- [9] K. L. Fuller, "To see and not be seen," *Proc. Inst. Elect. Eng. Radar and Signal Processing, F*, vol. 137, pp. 1–10, Feb. 1990.
- [10] P. E. Pace, *Detecting and Classifying Low Probability of Intercept Radar*. Norwood, MA: Artech House, 2004.
- [11] D. C. Schleher, "LPI radar: Fact or fiction," *IEEE Aerosp. Electron. Syst. Mag.*, vol. 21, pp. 3–6, May 2006.
- [12] E. J. Carlson, "Low probability of intercept (LPI) techniques and implementations for radar systems," in *Proc. IEEE National Radar Conf.*, Apr. 1988, pp. 56–60.
- [13] A. Denk, "Detection and jamming low probability of intercept (LPI) radars," Ph.D. dissertation, Naval Postgraduate School, Monterey, CA, 2006.
- [14] G. Lui, H. Gu, W. Su, and H. Sun, "The analysis and design of modern low probability of intercept radar," in *Proc. CIE Int. Conf. on Radar*, Oct. 2001, pp. 120–124.
- [15] P. Wu, "On sensitivity analysis of low probability of intercept (LPI) capability," in *Proc. IEEE Military Communications Conf.*, Oct. 2005, vol. 5, pp. 2889–2895.
- [16] K. E. Olsen, T. Johnsen, S. Johnsrud, R. Gundersen, H. Bjordal, I. Tansem, and P. Sornes, "Results from an experimental continuous wave low probability of intercept bistatic radar – The first steps toward multistatic radar," in *Proc. Int. Radar Conf.*, 2003, pp. 288–292.
- [17] N. Levanon and B. Getz, "Comparison between linear FM and phase-coded CW radars," *Proc. Inst. Elect. Eng.—Radar, Sonar, Navigation*, vol. 141, no. 4, pp. 230–240, Aug. 1994.
- [18] A. G. Stove, "Linear FMCW radar techniques," *Proc. Inst. Elect. Eng. F*, vol. 139, no. 5, pp. 343–350, Oct. 1992.
- [19] B. E. Anderson, M. Persson, and K. Boman, "FMCW and super resolution techniques applied to an LPI short range air search radar," in *Proc. Radar 97*, Oct. 1997, pp. 406–410.
- [20] F. Gross and K. Chen, "Comparison of detectability of traditional pulsed and spread spectrum radar waveforms in classic passive receivers," *IEEE Trans. Aerosp. Elect. Sys.*, vol. 41, no. 2, pp. 746–751, Apr. 2005.
- [21] J. Vankka, "Digital frequency synthesizer/modulator for continuous-phase modulation with slow frequency hopping," *IEEE Trans. Veh. Technol.*, vol. 46, no. 4, pp. 933–940, Nov. 1997.
- [22] M. Burgos-Garcia and J. Sanmartin-Jara, "A LPI tracking radar system based on frequency hopping," in *Proc. Int. Radar Symp.*, Munich, Germany, Sep. 1998, pp. 151–159.
- [23] G. Liu, H. Gu, W. Su, H. Sun, and J. Zhang, "Random signal radar – A winner in both the military and civilian operating environments," *IEEE Trans. Aerosp. Elect. Systems.*, vol. 39, no. 2, pp. 489–498, Apr. 2003.
- [24] Y. Shirman, S. Leshchenko, and V. M. Orlenko, "Advantages and problems of wideband radar," in *Proc. Int. Radar Conf.*, 2003, pp. 15–21.
- [25] E. J. Baghdady, "Directional signal modulation by means of switched spaced antennas," *IEEE Trans. Commun.*, vol. 38, no. 4, pp. 399–403, Apr. 1990.
- [26] W. D. Wirth, "Omni-directional low probability of intercept radar," in *Proc. Int. Conf. on Radar*, Paris, 1989, pp. 25–30.
- [27] W. D. Wirth, "Long term coherent integration for a floodlight radar," in *Proc. IEEE Int. Radar Conf.*, May 1995, pp. 698–703.
- [28] W. D. Wirth, *Radar Techniques Using Array Antennas*. London, U.K.: IET, 2001.
- [29] G. Binias, "Target track extraction procedure for OLPI antenna data on the basis of Hough transforms," *IEE Proc. Radar Sonar Navig.*, vol. 149, pp. 29–32, Feb. 2002.
- [30] G. Brown, C. Kerce, and M. Mitchell, "Extreme beam broadening using phase only pattern synthesis," in *IEEE Sensor Array and Multi-channel Sig. Processing Workshop Proc.*, 2006, pp. 36–39.
- [31] R. Kinsey, "Phased array beam spoiling technique," in *IEEE Antennas Propag. Society AP-S Int. Symp.*, 1997, vol. 2, pp. 698–701.
- [32] E. Bayliss, "Phase synthesis technique with application to array beam broadening," in *IEEE Antennas Propag. Digest*, 1966, pp. 427–432.
- [33] S. Srinivasa and S. Jafar, "The optimality of transmit beamforming: A unified view," *IEEE Trans. Inf. Theory*, vol. 53, no. 4, pp. 1558–1564, Apr. 2007.



Daniel E. Lawrence (S'98–M'02) received the B.E.E. and M.S. degrees in electrical engineering from Auburn University, Auburn, AL, in 1996 and 1998, respectively, and the Ph.D. degree in electrical engineering from the University of Michigan, Ann Arbor, in 2002.

In 2002, he joined the Phase IV Systems Operation of Technology Service Corporation, Huntsville, AL and serves as a Subject Matter Expert in the area of radar and communication systems for a wide range of defense programs. He also serves as a part-time instructor with the Department of Electrical Engineering, University of Alabama in Huntsville, teaching both undergraduate and graduate courses in radar, antennas, and signal processing. His current research interests include low-probability of intercept radar techniques, high fidelity interferometric antenna design, electromagnetic scattering, and forward error correction techniques for robust missile communication links.